PHYSICAL REVIEW E VOLUME 48, NUMBER 4 OCTOBER 1993

Laser-produced carbon plasma in an ambient gas

Abhilasha, P. S. R. Prasad, and R. K. Thareja
Department of Physics and Centre for Laser Technology, Indian Institute of Technology, Kanpur 208 016, India
(Received 23 November 1992)

We report a detailed investigation of the double-peak structure in the temporal profile of the C II transition $3d\,^2D-4f\,^2F^o$ at 426.7 nm in a laser-produced carbon plasma at various air pressures. An estimate of the plasma expansion velocity from the temporal behavior at various distances from the target for C II, C III, and C IV species and electron density from the Stark broadened transition is also reported. It is proposed that the second peak in temporal profiles originates mainly due to stratification of the plasma into fast and slow ion components at the interface where the occurrence of the Rayleigh-Taylor instability causes deceleration of the laser plasma front by ambient gas.

PACS number(s): 52.50.Jm, 52.40.Nk, 52.25.−b, 52.20.−j

I. INTRODUCTION

The focused high-intensity laser radiation onto a solid target in vacuum or ambient gas creates a hot dense recombining plasma [1,2]. The interaction of an expanding plasma with an ambient background has been the subject of numerous experimental [3–5] and theoretical [6] investigations where it is shown that both plasma effects and atomic and molecular phenomena may play important roles in the formation of transient plasma. The studies are aimed at modeling various processes in space physics, plasma chemistry, and hydrodynamics of the expanding plasma. Laser-produced plasmas in metals in the presence of background gas have been used in the recombination phase for generation of laser oscillations [7,8] and as strong x-ray and vacuum ultraviolet sources [9,10]. Irons and co-workers [11–13] have reported detailed studies on the temporal, spatial, and spectral characteristics of ruby-laser-produced carbon plasma. In general, the nature of the interaction between laser plasma and ambient gas depends on parameters such as velocities of different ionic species, densities in the interaction region, ambient gas pressure, laser pulse width, etc. The influence of background gas pressure on the energy and angular distribution of ions [14,15] and the nature of interaction processes between the ions and the background gas particles has also been reported [16]. Laser-ablated carbon plasma in an ambient gas has been used for deposition of C_{60} on various substrates [17]. Ananlin *et al.* [18,19] have investigated the interaction of a laser plasma with the background gas in the pressure range 10^{-3}–1 Torr of air using spectroscopic and high-speed photographic methods.

In this paper we report on the studies of laser-produced carbon plasma in an ambient gas. We report an appearance of a peculiar double-peak structure in the temporal profile of the C II transition $3d\,^2D-4f\,^2F^o$ at 426.7 nm in a laser-produced carbon plasma as it expands into a background medium.

II. EXPERIMENTAL SETUP

The experimental setup used in the present study is similar to the one described elsewhere [20,21]. We used a Nd:YAG laser (DCR-4G) (where YAG denotes yttrium aluminum garnet) with Gaussian limited mode structure (1.06 μm) delivering 900 mJ of energy in 2.5 ns full width at half maximum with a repetition rate of 10 pulses/s to produce the carbon plasma. A 50-cm focal length lens focused the laser beam on to the graphite target to a spot of 240 μm diameter. The target was mounted in a vacuum chamber which could be evacuated to a pressure of $\leq 10^{-3}$ Torr. The experiment was carried out for different pressures in the range 10^{-3}–1 Torr, the background gas being air in our case. The target rod was continuously rotated and translated with an external motor so that each laser pulse falls on fresh graphite surface every time. The plasma radiation was imaged on to the entrance slit of monochromator (HRS-2, Jobin Yvon) with a lens of focal length of 12 cm so as to have one-to-one correspondence with the plasma and its image onto the slit of monochromator. The monochromator was continuously tuned using a microprocessor controlled scan system. The output from the monochromator was detected with a photomultiplier tube (1P28, Hamamatsu) and recorded on a strip chart recorder or displayed on the oscilloscope (11302A, Tektronics). The signals were digitized using digitizing video camera (Tektronics DCS 01) attached to the oscilloscope. Digitized signals were fed to personal computer for further data processing.

III. RESULTS AND DISCUSSION

The visible emission spectra of carbon plasma was recorded at different distances (z) away from the target surface by moving the monochromator in the horizontal plane in the direction perpendicular to the direction of the expanding plume. The emission lines were identified using the information available in the literature [22]. We have observed the transitions up to C V species. The electron temperature was estimated from relative intensities [20,23] of C II species originating from $n=4$ excited states. Various parameters for electron temperature are available in the literature [22]. The electron temperature for C II species at 8 mm from the target is estimated to be ~ 2 eV when pressure of the chamber was better than 10^{-3} Torr. The electron density is estimated from the

Stark broadened [24] profile of the C II transition $3p\,^2p^o{-}4s\,^2S$ at 392.0 nm. Various parameters for electron density are available in the literature [23]. Line profile was recorded by keeping the monochromator resolution to maximum (0.02 nm). The observed line shape was fitted with a Lorenzian shape whose true half width is given by [24]

$$\Delta\lambda = 2W\left[\frac{N_e}{10^{16}}\right]\text{Å} \tag{1}$$

where W is electron impact parameter which can be interpolated to different temperatures and N_e is electron density. A typical Stark broadened profile of the C II transition at 392.0 nm at a distance of 8 mm away and parallel to the target surface when pressure of the chamber was better than 10^{-3} is shown in Fig. 1. Using Eq. (1) the estimated electron density at a distance of 8 mm from the target surface is 5×10^{16} cm^{-3}. In order to estimate densities at various pressures, the variation of a Stark broadened profile with pressure of the background gas was also carried out.

Temporal profiles were recorded of the transitions $3d\,^2D{-}4f\,^2F$ at 426.7 nm of C II, $3s\,^3S{-}3p\,^3P^o$ at 465.0 nm of C III, and $3s\,^2S{-}3p\,^2P^o$ at 580.1 nm of C IV at different distances from and parallel to the target to estimate the velocities of different species. Figure 2 shows the variation of delay in the peak intensities with a distance from the target at background gas pressure of 10^{-3} Torr and a slope of the curve gives the velocity of the plasma front. The expansion velocities of C II, C III, and C IV species are found to be about 4×10^6, 7×10^6, and 10×10^6 cm/s, respectively. It is observed that expansion velocity decreases with decrease in ionic charge from C IV to C II.

The spatial and temporal characteristics of various ionic states at various pressures of air in the chamber were

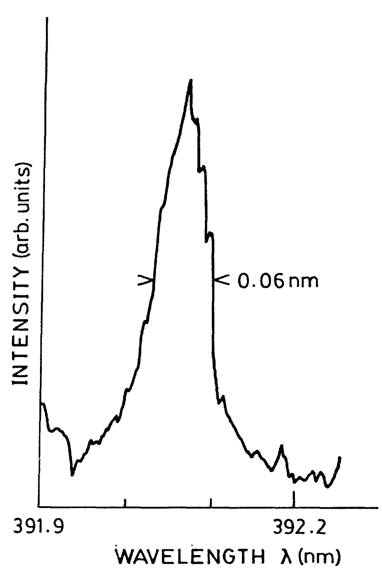

FIG. 1. Typical stark broadened profile of C II transition $3p\,^2P^o{-}4s\,^2S$ at 392.0 nm for 1.06-μm irradiation at pressure $\sim10^{-3}$ Torr.

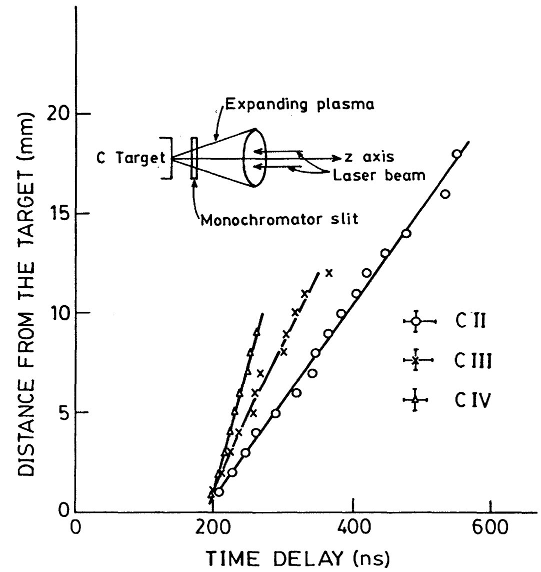

FIG. 2. Variation of time delay in the peak intensities with distance from the target for 1.06-μm irradiation when the pressure is less than 10^{-3} Torr. Circles: C II transition $(3d\,^2D{-}4f\,^2F^o)$ at 426.7 nm. Crosses: C III transition $(3s\,^3S{-}3p\,^3P^o)$ at 465.0 nm. Triangles: C IV transition $(3s\,^2S{-}3p\,^2P^o)$ at 580.1 nm. Inset shows the expanding plasma from the monochromator slit viewpoint.

performed. An interesting feature observed is the appearance of a hump in the temporal profile for the transition $3d\,^2D{-}4f\,^2F^o$ of C II at 426.7 nm at distances far away from the target surface ($z>8$ mm) at pressure equal to or better than 10^{-3} Torr in the chamber. A single peak is observed for distance less than 8 mm. On increasing pressure in the chamber the hump takes a very distinct shape and the profile appears as a double-peak structure at 0.1 Torr. A further increase in background pressure decreases the onset distance for the double-peak structure. Figure 3 shows the effect of air pressure in the chamber on the shape of the temporal profiles at 0.1 and 1 Torr pressure. The second peak appears at a distance of 8 and 5 mm, respectively, from the target at 0.1 and 1 Torr air pressure. The variation of delay in the peak intensities for the first and second peak at different distances from the target for various pressures is plotted in Fig. 4. The slope of the curve shows that second peak decelerates and the first peak accelerates with the increase in pressure. It is worthwhile to mention that no such peak was observed for C III and C IV species. However, for C I transition $2p^2\,^1S{-}3s\,^1P^o$ at 247.9 nm, we observed a fast and a slow component of the neutral species at low pressures (10^{-2} Torr), but no change in the structure was observed with an increase in air pressure up to 1 Torr. It is similar to the double-peak structure reported by Dixon, Elton, and Seely [16,25] in helium atmosphere (1–10 Torr). Our observation of the double-peak structure of the C II species is quite different from that of the C I species; the appearance of the second peak depends on background gas pressure and the onset distance for second peak also decreases with increase in background gas pressure. Our observation does not follow the classical blast wave model [26].

In general, the existence of the above structure could originate from processes such as (a) electron-ion recombination interactions with in the plasma, (b) collisional interactions between the expanding ions and ambient gas molecules, and (c) stratification of the plasma due to instabilities occurring at the interface between laser plasma and the ambient gas. To explain our observation, now we discuss each one of the three possibilities. The recombination process can occur either due to the radiative or three-body recombination [27]. The functional dependence of the recombination rate for the radiative and the three-body recombination on the ion charge $\bar{Z}$, electron density n_e, ion density n_i, and electron temperature T_e is $n_e n_i \bar{Z}^2 T_e^{-3/4}$ and $n_e^2 n_i \bar{Z}^3 T_e^{-9/2} \ln\sqrt{\bar{Z}^2+1}$, respectively. The calculations of recombination rate coefficients show that radiative recombination is a dominant process close to the target surface and three-body recombination process is dominant beyond a few millimeters from the target [27]. Rate coefficients for three-body recombination and other interaction processes are calculated which indicate that three-body recombination is not a dominant phenomenon in comparison to other processes. The interaction processes such as collisional charge transfer

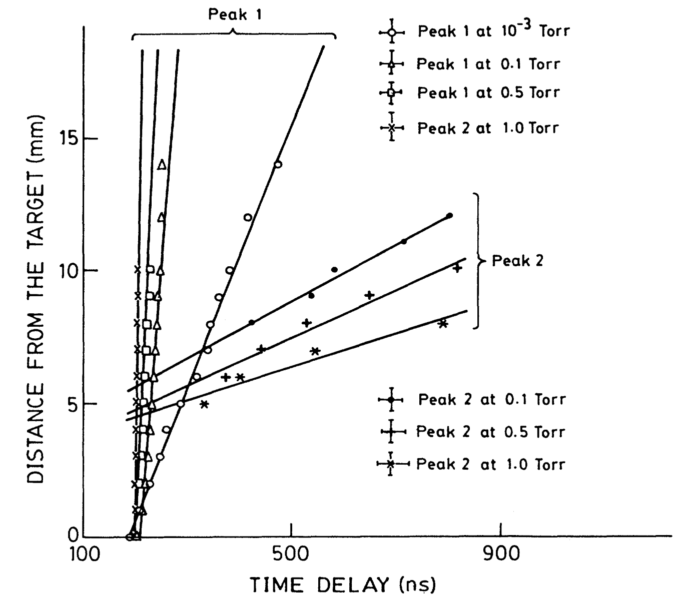

FIG. 4. Variation of time delay in the peak intensities for the first and second peak at different distances from the target surface for various pressures.

occurring due to interaction of target ions and background gas may play an important role.

The double-peak structure is pronounced for the C II transition originating from $n=4$ excited state at 426.7 nm; the effect is not observed for the transitions at 407.4 and 588.9 nm. Dixon and Elton [25] have shown that resonance charge-transfer process is a velocity-dependent one. In our experiment, we find that the faster components have velocities an order of magnitude less than that reported by Dixon and Elton which makes the resonance charge-transfer process a less probable one in our case. We also observed the double-peak structure from lines originating at $n=2$ and 3 levels, respectively, at 251.2 and 283.7 nm. Thus the phenomenon of the double-peak structure cannot be explained on the basis of electron-ion recombination and charge-transfer process. Collisionless interactions are neglected as they are mainly important only at smaller distances.

The shape of the expanding plasma was also observed visually to look for any changes in the pattern of expanding plume. At low pressure less than 10^{-3} Torr, the expanding plume is smooth. As the pressure increases the plasma front breaks up and forms a separate luminous region which eventually becomes bracket shaped, a shape similar to an irregular sickle. Visual observations at a background gas pressure of 0.1 Torr can well be compared with Ananlin *et al.* [19] where they explained the onset of micro-instability using high-speed photography at 0.26 Torr of air pressure as evidenced by the asymmetric luminous region having the structure similar to a bracket in the expanding plasma (Figs. 2 and 3 of Ref. [19]). Accordingly, the increase in growth of instability was evidenced by the increase in intensity and dimensions of bracket shape structure. In our case, the increase in the number of peaks at the plasma front with pressure

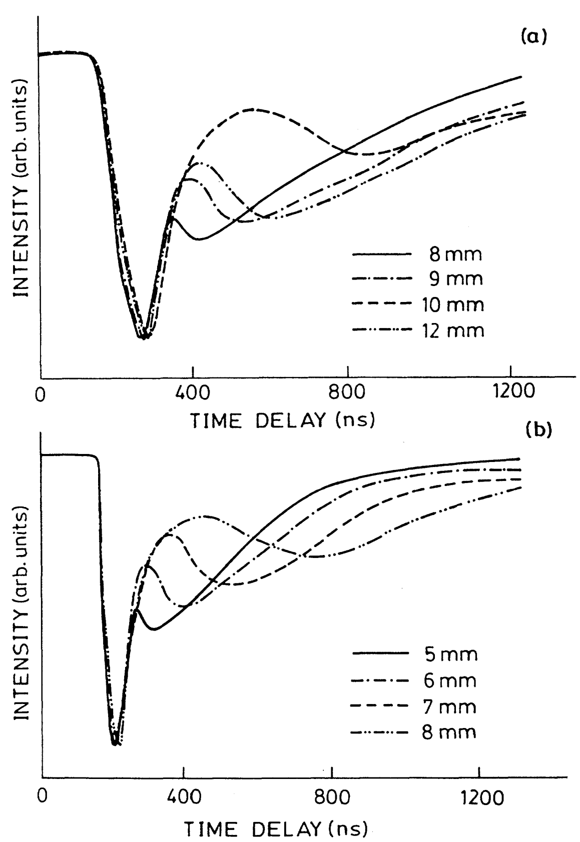

FIG. 3. Influence of the background gas (air) pressure on the shape of the temporal profiles of C II transition $3d\ ^2D-4f\ ^2F^o$ at 426.7 nm at pressures of (a) 0.1 and (b) 1 Torr and at different distances from the target surface.

signifies the increase in growth of turbulence. At pressures less than 10^{-3} Torr, plasma is fairly homogeneous in its structure. The inhomogeneities of the laser power density in the laser-focused spot [28,29] can give rise to fast and slow ion components near the target surface. Separation of the two components close to the target surface is not observed in our case. We observe that at low pressures less than 10^{-3} Torr, the density of plasma ions decreases largely due to expansion and fast recombination processes resulting in mutual penetration of the plasma and the gas. During interpenetration, the transfer of kinetic energy from the laser plasma to the background gas takes place and energy and momentum exchange occurs as a result of ion-ion Coulomb scattering, ion-neutral collisions, charge-transfer interactions, etc. When pressure is increased to 10^{-2} Torr, the interaction region shifts towards the target due to increased density of ambient gas. At a pressure of ~ 0.1 Torr, mutual penetration of the laser plasma ions and the ambient gas decreases and interaction region becomes narrower, thus forming an interface. Near the interface the instabilities such as Rayleigh-Taylor sets in the plasma. Furthermore, density fluctuations in the interface region leads to deceleration of laser plasma front. Due to interface formation and density fluctuations, stratification effect in the plasma increases where fast component penetrates the ambient gas and slow one decelerates due to appearance of instability and consequently gives rise to a distinct double-peak structure in temporal profiles of C II transition at 426.7 nm at about 8 mm from the target. The growth of the Rayleigh-Taylor instability [30–32] can be expressed as

$$n^2 = Ka\frac{(\rho_2 - \rho_1)}{(\rho_2 + \rho_1)} \tag{2}$$

where ρ_2 the density of the ambient gas, ρ_1 the density of the laser plasma, and a is the acceleration of the interface. Now if $\rho_2 < \rho_1$, the interface is stable while if $\rho_2 > \rho_1$, the arrangement is unstable. The growth of instability occurs in the maximum acceleration region, which can be estimated from the derivative of momentum-conservation equation

$$\frac{d}{dt}[(M_0 + \tfrac{4}{3}\pi R^3 \rho_2)u] = 0 , \tag{3}$$

where M_0 is the laser plasma mass, u is plasma front velocity, and R is the distance from the target. The solution of Eq. (3) yields

$$\rho_2 = \frac{6M_0}{28\pi R^3} \tag{4}$$

where R is the distance from the target where acceleration is maximum and interface formation occurs. Using our experimental parameters, viz. $R \simeq 8$ mm, where the distinct double-peak structure occurs and $M \simeq 10^{-6}$ g, gives $\rho_2 = 1.3 \times 10^{-7}$ g/cm^3, which corresponds to the air pressure of 0.16 Torr, close to the our experimental value of 0.1 Torr. Using the estimated density of the laser plasma ions we find that at lower pressures, $\rho_1 > \rho_2$ in the interaction region whereas at higher pressures $\rho_2 \geq \rho_1$ and acceleration is negative. Also it follows from Eq. (2) that $n^2 > 0$ at lower pressures whereas $n^2 < 0$, in agreement with the condition for the growth of the instability at 0.1 Torr. Since the densities of the higher ionic species of carbon, i.e., C III and C IV, ions decrease rapidly with distance due to radiative recombinations occurring in the plasma, no hump and double-peak structure are observed in these species.

IV. CONCLUSIONS

From double-peak structure in temporal profiles of the C II transition $3d\,^2D - 4f\,^2F^o$ at 426.7 nm, an investigation of the transition from mutual penetration to interface formation between carbon ions and background gas is reported. At the interface region due to density fluctuations, Rayleigh-Taylor instability occurs in the decelerating laser plasma front which leads to stratification of the plasma. Pressure at which Rayleigh-Taylor instability occurs at the interface is estimated theoretically which compares well with our experimental observation.

[1] J. M. Dawson, Phys. Fluids **7**, 981 (1964).

[2] P. K. Carroll and E. T. Kennedy, Contemp. Phys. **22**, 61 (1984).

[3] D. W. Koopman, Phys. Fluids **14**, 1707 (1971)

[4] S. O. Dean, E. A. Mclean, J. A. Stamper, and H. R. Griem, Phys. Rev. Lett. **27**, 487 (1971).

[5] O. B. Ananlin, Yu. A. Bykovskii, E. L. Stupitskit, and A. M. Khudaverdyan, Kvant. Elektron. (Moscow) **14**, 2313 (1987) [Sov. J. Quantum Electron. **17**, 1474 (1987)].

[6] T. P. Wright, Phys. Rev. Lett. **28**, 268 (1972).

[7] W. T. Silfvast, L. H. Szeto, and O. R. Wood II, Opt. Lett. **4**, 271 (1979).

[8] R. H. Dixon, J. F. Seely, and R. C. Elton, Phys. Rev. Lett. **40**, 122 (1978).

[9] J. M. Bridges, C. L. Cromer, and T. J. Mcllrath, Appl. Opt. **25**, 2208 (1986).

[10] V. I. Bayanov, V. A. Serebryakov, I. Yu. Skobelev, N. A. Soloev, A. Ya. Faenov, and S. Ya. Khakhalin, Kvant. Elektron. (Moscow) **15**, 1842 (1988) [Sov. J. Quant. Electron. **18**, 1150 (1988)].

[11] F. E. Irons, R. W. P. McWhirter, and N. J. Peacock, J. Phys. B **5**, 1975 (1972).

[12] B. C. Boland, F. E. Irons, and R. W. P. McWhirter, J. Phys. B **1**, 1180 (1968).

[13] M. Galanti and N. J. Peacock, J. Phys. B **8**, 2427 (1975).

[14] R. M. Clement, R. A. Davies, H. T. Miles, and S. K. Sethuramman, J. Phys. D **13**, 1643 (1980).

[15] J. Farny, S. Nagraba, and E. Woryna, J. Tech. Phys. **28**, 185 (1987); K. Mann and K. Rohr, Laser Part. Beams **10**, 435 (1992).

[16] R. H. Dixon, R. C. Elton, and J. F. Seely, Opt. Commun. **45**, 397 (1983).

[17] G. Meijer and D. S. Bethune, J. Chem. Phys. **93**, 7800 (1990).

[18] O. B. Ananlin, Yu. A. Bykovskii, B. V. Zamyshlyaev, A. G. Guz, E. L. Stupitski, and A. M. Khudaverdyan, Fiz. Plazmy **9**, 319 (1983) [Sov. J. Plasma Phys. **9**, 186 (1983)].

[19] O. B. Ananlin, Yu. A. Bykovskii, Yu. V. Eremin, E. L. Stupitskii, I. K. Novikov, and S. P. Frolov, Kvant. Elektron. (Moscow) **18**, 869 (1991) [Sov. J. Quantum Electron. **21**, 787 (1991)].

[20] R. Tambay, R. Singh, and R. K. Thareja, J. Appl. Phys. **72**, 1197 (1992).

[21] V. Kumar and R. K. Thareja, J. Appl. Phys. **67**, 3260 (1990).

[22] A. R. Striganov and N. S. Sventitskii, in *Tables of Spectral Lines of Neutral and Ionized Atoms* (Plenum, New York, 1968). W. L. Wiese, M. W. Smith, and B. M. Glennon, *Atomic Transition Probabilities Vol. I,* Natl. Bur. Stand. Ref. Data Ser. Natl. Bur. Stand. (U.S.) Circ. No. 4 (U.S. GPO, Washington, DC, 1966).

[23] H. R. Griem, *Plasma Spectroscopy* (McGraw-Hill, New York, 1964).

[24] G. Bekefi, *Principles of Laser Plasmas* (Wiley, New York, 1976).

[25] R. H. Dixon and R. C. Elton, Phys. Rev. Lett. **38**, 1072 (1977).

[26] T. P. Hughes, *Plasmas and Laser Light* (Wiley, New York, 1975), p. 435.

[27] P. T. Rumsby and J. W. M. Paul, Plasma Phys. **16**, 247 (1974).

[28] P. Mulser, Plasma Phys. **13**, 1007 (1971).

[29] R. R. Goforth and P. Hammerling, J. Appl. Phys. **47**, 3918 (1976).

[30] S. Chandrasekhar, *Hydrodynamic and Hydromagnetic Stability* (Oxford University Press, London, 1981), Chap. X, p. 428.

[31] M. Mitchner and R. K. M. Landshoft, Phys. Fluids **7**, 862 (1964).

[32] G. Taylor, Proc. R. Soc. London Ser. A **201**, 192 (1950).